RSC Advances

ROYAL SOCIETY OF CHEMISTRY

www.rsc.org/advances

ARTICLE

Formation and Chemistry of Carboxylic Anhydrides at the Graphene Edge

Martin Rosillo-Lopez,[a] Tai Jung Lee,[a] Malika Bella,[b] Martin Hart,[a] and Christoph G. Salzmann[a],[*]

Using graphene for a wide range of applications often requires delicate chemical processing and functionalisation. Here we first report the synthesis of graphene nanoflakes with carboxylic acid groups at the graphene edges from multi-wall carbon nanotube materials. Using this material we then show that highly reactive carboxylic anhydride groups exist in dynamic equilibrium with the carboxylic acids in aqueous dispersion. Heating in vacuum shifts the equilibrium as about 80% of the carboxylic acid groups transform to the anhydrides. These new insights into graphene chemistry enable us to develop a simple, straight-forward chemical functionalisation protocol for graphene making use of the anhydrides. The graphene nanoflakes were found to react readily with amine nucleophiles in aqueous dispersion to yield the corresponding amides. The new protocol allows us to alter the zetapotential of the graphene nanoflakes and to decorate the graphene edges with gold nanoparticles. Due to its simplicity, we expect this procedure to find wide-spread use in the chemical functionalisation of graphene and to enable new graphene-based applications.

Introduction

Graphene, a single layer of graphitic carbon, displays highly remarkable physical properties such as mechanical stability,[1] optical transparency,[2] impermeability,[3] and electrical[4] and thermal conductivity.[5] Chemical processing and functionalisation are often required to use graphene in applications as diverse as drug delivery,[6, 7] photovoltaic[8, 9] and electronic devices,[10] energy storage[11-13] and chemical sensors.[14-16] The chemistry of graphene is remarkably complex and some aspects, such as the chemical structure of graphene oxide, are even controversial.[17, 18] Graphene chemistry can be divided with respect to the locus of chemical functionalisation, *i.e.* either on the basal plane[19] or at the edge which typically relies on carboxylate chemistry. Current standard procedures are carbodiimide-catalysed[20-22] or proceed *via* acid chlorides.[22-25]

Despite much progress in the structural characterisation of graphene and its edges,[26, 27] the characterisation tools for chemically functionalised graphenes are often not able to reveal the exact chemical nature and location of functional groups. The purification of products materials can also be difficult as it is often impossible to completely remove all reagents or other impurities from chemically functionalised graphene. Further progress in graphene chemistry and simple

protocols for chemical functionalisation are therefore urgently needed.

Here we first report the bulk preparation of carboxylated graphene nanoflakes (*cx*-GNFs) from readily available chemical vapour deposition (CVD) multi-wall carbon nanotube materials (Fig. 1a). The material is then used to explore the chemistry of the carboxylated graphene edge and the chemical properties of the *cx*-GNFs are benchmarked against the widely-used graphene oxide (GO). The aim is to develop new procedures for the facile chemical functionalisation of the graphene edge.

Our new preparation procedure for *cx*-GNFs relies on the oxidative break-down of CVD multi-wall carbon nanotube material in a first step with a 3:1 vol% mixture of concentrated sulfuric and nitric acid. The separation of the *cx*-GNFs from the large amounts of the inorganic acids is achieved by neutralisation with KOH pellets which leads to precipitation of K_2SO_4 and KNO_3 while the *cx*-GNFs remain in dispersion (Fig. 1b). The remaining dissolved salts in the *cx*-GNF dispersion are then removed by dialysis and the pure *cx*-GNF material is obtained after freeze-drying in 16 w% yield (further details are provided in the ESI†).

The purity of the *cx*-GNFs is illustrated by the survey X-ray photoelectron spectrum in Fig. 1c which shows no other elements than carbon and oxygen. A high-resolution spectrum of the C1s region confirms the presence of sp^2 carbon with a peak centred at 285.3 eV as well as a lower intensity peak at 289.4 eV which is attributed to carbon in oxidation state +III such as in carboxyl (COOH) groups.[25, 28]

Comparison with the C1s region of GO highlights that the *cx*-GNFs are a very different carbon nanomaterial. The most pronounced peak of GO is located at 287.2 eV which is due to alcohol and epoxide groups on the GO basal plane.[28] COOH

[a.] *University College London, Department of Chemistry, 20 Gordon Street, WC1H 0AJ London, UK. E-mail:c.salzmann@ucl.ac.uk*
[b.] *Durham University, Department of Chemistry, South Road, Durham DH1 3LE, UK*

RSC Advances Accepted Manuscript

groups are present in very small quantities as illustrated by the low spectral intensity at around 290 eV. Thermal annealing at 900°C in a high vacuum leads to removal of oxygen-containing groups for both the *cx*-GNFs and the GO as shown by the second inset in Fig. 1c.
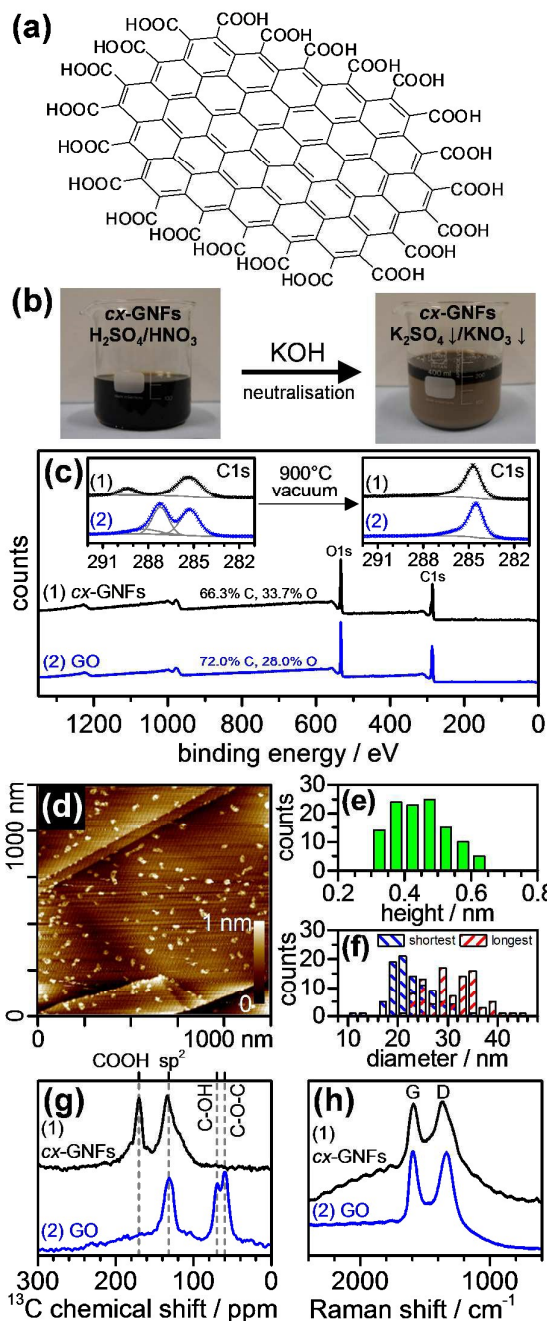
Fig. 1 Chemical composition and structure of *cx*-GNFs. (a) Idealised chemical structure of a small *cx*-GNF. (b) Photographic images of the filtered reaction mixture before and after neutralisation. (c) X-ray photoelectron spectra of *cx*-GNFs and GO. The insets show the C1s region before and after heating to 900°C under high vacuum. (d) Atomic force microscopy image of *cx*-GNFs spin-coated onto highly oriented pyrolytic graphite. (e) Height and (f) diameter distribution of the *cx*-GNFs. (g) ^{13}C solid-state NMR and (h) Raman spectra of *cx*-GNFs and GO.

The atomic force microscopy image in Fig. 1d shows *cx*-GNFs spin-coated from aqueous dispersion onto highly-oriented pyrolytic graphite. The average height of the *cx*-GNFs is 0.45 nm which is the expected value for monolayer graphene (Fig. 1e).[25] The averages of the shortest and longest lateral diameters are 22.5 and 30.8 nm, respectively (Fig. 1f). Similar dimensions have also been found using transmission electron microscopy (Fig. S8†). The *cx*-GNFs are therefore one to two orders of magnitude smaller than a typical GO sheet.

Consistent with the XPS results, the ^{13}C solid-state NMR spectrum of *cx*-GNFs shown in Fig. 1g indicates the presence of sp^2 carbon and carboxylic acids, and the absence of alcohol and epoxide groups which are characteristic for GO.[29] The Raman spectra of *cx*-GNFs and GO on the other hand are quite similar which may indicate that the graphenic regions within our GO are of similar dimensions as the *cx*-GNFs (Fig. 1h).

The availability of highly carboxylated nanographenes now enables us to explore the chemical properties of COOH groups at the graphene edge. We first show that they can transform to the corresponding carboxylic anhydrides with the elimination of water upon heating in vacuum according to the reaction scheme shown in Fig. 2a.

ARTICLE
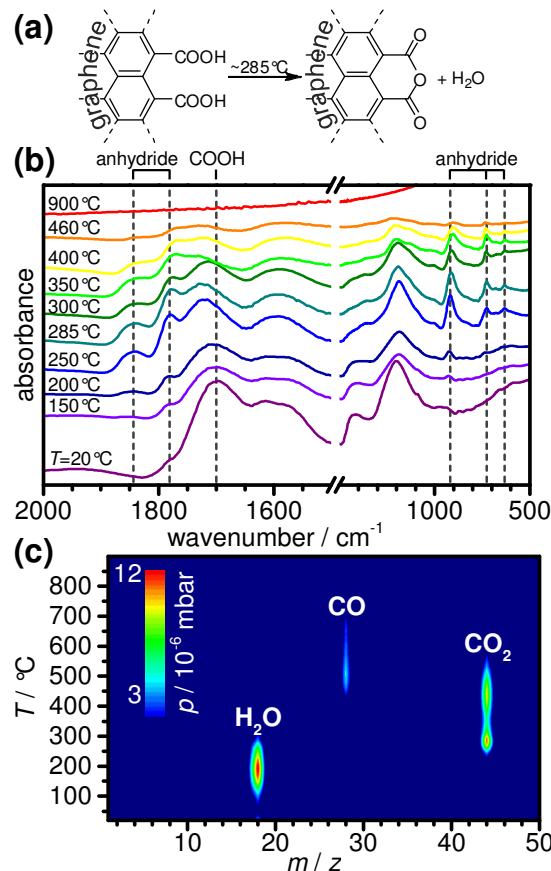
Fig. 2 Formation of carboxylic anhydrides upon heating *cx*-GNFs in high vacuum. (a) Reaction scheme of the anhydride formation. (b) FT-IR spectra of *cx*-GNFs after heating to the indicated temperatures. (c) In-situ mass spectrometry of desorbing gas species upon heating.

The formation of carboxylic anhydrides is illustrated by the FT-IR spectra in Fig. 2b. The as-made *cx*-GNFs show an intense peak centred at ~1700 cm^{-1} which is the expected value of the C=O stretching mode of COOH groups.[25, 28] Upon heating in vacuum new C=O stretching peaks emerge at 1781 and 1844 cm^{-1} at the expense of the COOH peak. These two frequencies are indicative for cyclic carboxylic anhydrides and correspond to the asymmetric and symmetric C=O stretching modes, respectively.[28] The conversion of the COOH groups to the anhydride is, however, not fully quantitative which may be due to geometric constraints at the graphene edge such as 'stranded' COOH groups located either between anhydride groups or spatially too distant from other COOH groups so that cyclic anhydrides cannot form. The intensity of the COOH peak decreases markedly above 250°C. However, this does not lead to a further increase of the intensities of the anhydride peaks and is therefore correlated with the thermal decomposition of the 'stranded' COOH groups. The anhydride groups are thermally more stable. However, heating to 460°C leads to almost complete disappearance of the anhydride C=O stretching peaks as well as the peaks characteristic for anhydrides in the 500 to 1000 cm^{-1} range. Consistent with the XPS data shown in Fig. 1c heating to 900°C finally shows the absence of polar functional groups.

Mass-spectrometry data recorded upon heating *cx*-GNFs in vacuum corroborate the results from FT-IR spectroscopy (Fig. 2c). Water is released first upon heating. Detailed analysis of the H$_2$O desorption profile suggests that more than 90% of the desorbing water is physisorbed. A second water loss, attributed to anhydride formation, starts at about 200°C (Fig. S6a†). This is followed by two separate decarboxylation processes with maxima at about 280 and 440°C, respectively. According to the FT-IR measurements, the first corresponds to the decarboxylation of the 'stranded' COOH groups and the second to the release of CO$_2$ due to thermal decomposition of carboxylic anhydrides. Peak fitting of the CO$_2$ desorption profile shows that about 81% of the COOH groups present in *cx*-GNFs form anhydrides upon heating (Fig. S6b†). Decarbonylation, the loss of CO, takes place last which is consistent with the thermal decomposition pattern of other carboxylic anhydrides.[30] The overall thermal decomposition pattern is consistent with what has been observed for aromatic polycarboxylic acids.[31] For example, benzene-1,2,3-tricarboxylic acid releases water at 190°C due to anhydride formation followed by decarboxylation of the remaining COOH group at 300°C to give phthalic anhydride.[31]

The thermal decomposition of GO is very different in comparison. Simultaneous desorption of H$_2$O, CO and CO$_2$ is observed at about 250°C (Fig. S7†) again illustrating that the *cx*-GNFs and GO are very different materials.

Formation and decomposition reactions of carboxylic anhydrides have previously been discussed in the context of chemically functionalised activated carbons.[32, 33] However, these investigations were complicated by the chemically diverse nature of activated carbons.
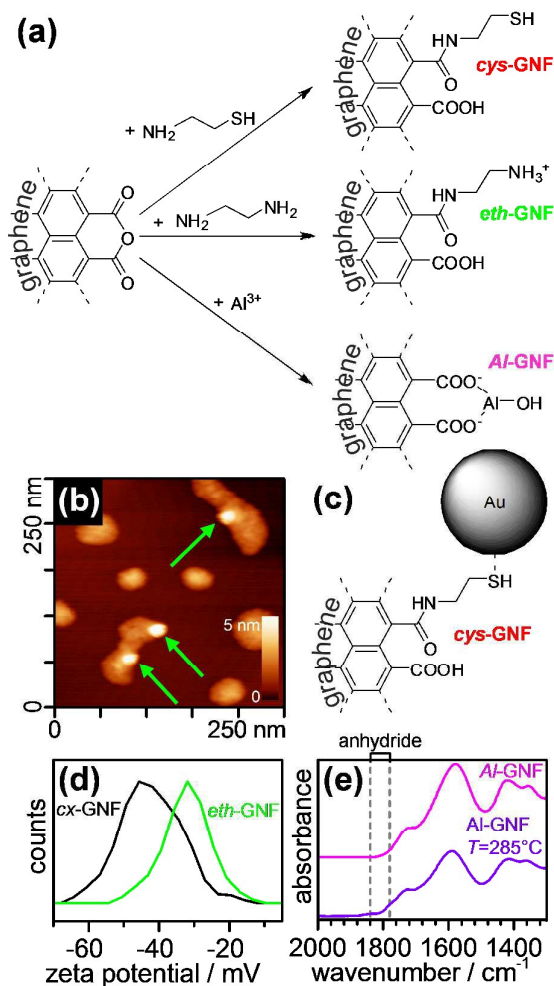
Fig. 3 Chemical functionalisation of *cx*-GNFs via the anhydride. (a) Reaction scheme of an anhydride with cysteamine, ethylene diamine and Al^{3+} cations. (b) AFM image and (c) chemical structure of the coordination of gold nanoparticles to cysteamine functionalised GNFs. (d) Change in zeta-potential upon functionalisation with ethylene diamine. (e) FT-IR spectra of Al-functionalised GNFs before and thermal treatment in vacuum.

The presence of carboxylic anhydride groups at the graphene edge offers an exciting prospect for simple chemical functionalisation due to their highly reactive chemical nature. Alongside acid chlorides, carboxylic anhydrides are the most reactive carboxylic acid derivatives and therefore highly susceptible for nucleophilic attack at the electropositive carbonyl carbon atoms. The reactive nature of the anhydride groups after heating in vacuum is illustrated by the hydrolysis

reaction in water and even humid air at room temperature back to the carboxylic acids (Fig. S9†).

Yet, close inspection of the FT-IR spectra shown in Figs 2b and S9† shows that the as-made *cx*-GNF material as-well as the hydrolysed material display a weak intensity of the lower wavenumber C=O stretching peak characteristic for anhydrides. This suggests that a small fraction of the COOH groups already form anhydrides before the equilibrium is shifted by heating in vacuum and that a small fraction of anhydride groups remains after hydrolysing the vacuum-heated material.

We next show that carboxylic anhydrides exist in dynamic equilibrium in aqueous dispersions of *cx*-GNFs by reacting them with amine nucleophiles. Fig. 3a shows the reaction schemes of an anhydride group with cysteamine or ethylenediamine to give the chemically functionalised *cys*-GNF and *eth*-GNF product materials, respectively. The reactions yield the corresponding amides plus a free COOH group which can then in principle form another anhydride leading to a 'cascade of chemical functionalisation' along the carboxylated graphene edge.

XPS and FT-IR spectra indicating the successful chemical functionalisation of the *cx*-GNFs are shown in Figs S3-5†. The AFM picture in Fig. 3b shows that the chemical functionalisation with cysteamine has, as expected, taken place at the graphene edges as 5 nm gold nanoparticles coordinate to the thiol groups of *cys*-GNF according to Fig. 3c.

The zetapotential measurements shown in Fig. 3d show that the as-made *cx*-GNFs display an average zetapotential of about -45 mV due to negatively charged carboxylates which are in equilibrium with carboxylic acids. The chemical functionalisation of *cx*-GNFs with ethylene diamine shifts the zetapotential to about -30 mV as positively charged NH_3^+ groups are introduced.

In addition to using the anhydride groups for chemical functionalisation we also show how their formation can be suppressed. This is achieved with Al^{3+} cations which are known to form some of the strongest complexes with carboxylates.[34] The *Al*-GNF material consequently does not show the anhydride peaks in the FT-IR spectra even after vacuum heating to 285°C (Fig. 3e).

Conclusions

In summary, we have opened up a new chapter in graphene chemistry by showing that carboxylic anhydride groups exist in dynamic equilibrium at highly carboxylated graphene edges. This was used to develop a simple single-step protocol for chemical functionalisation of graphene. We anticipate that the new procedure will be used extensively for, for example, creating graphene building blocks for the development of new self-assembly approaches or linking amine-containing biomolecules, such as proteins or enzymes, to graphene for medical and energy-related applications.

Acknowledgements

Notes and references

1. C. Lee, X. Wei, J. W. Kysar and J. Hone, *Science*, 2008, **321**, 385-388.
2. K. Loh, Q. Bao, G. Eda, M. Chhowalla, Q. Loh, G. Bao and M. Eda, *Nat. Chem.*, 2010, **2**, 1015-1024.
3. J. S. Bunch, S. Verbridge, J. Alden, A. M. van der Zande, J. Parpia, S. S. Verbridge, H. Craighead and P. McEuen, *Nano. Lett.*, 2008, **8**, 2458-2462.
4. I. Meric, M. Han, A. Young, B. Ozyilmaz, P. Kim, K. Shepard, M. Meric, A. Han, B. Young, P. Ozyilmaz and K. Kim, *Nat. Nanotechnol.* , 2008, **3**, 654-659.
5. A. Balandin, S. Ghosh, W. Bao, I. Calizo, D. Teweldebrhan, F. Miao, S. Balandin, W. Ghosh, I. Bao, D. Calizo, F. Teweldebrhan and C. Miao, *Nano. Lett.*, 2008, **8**, 902-907.
6. J. Liu, L. Cui and D. Losic, *Acta Biomater.*, 2013, **9**, 9243-9257.
7. S. Goenka, V. Sant and S. Sant, *J. Control. Release*, 2014, **173**, 75-88.
8. G. Eda, Y.-Y. Lin, S. Miller, C.-W. Chen, W.-F. Su and M. Chhowalla, *Appl. Phys. Lett.*, 2008, **92**, 233305.
9. D. W. Chang, H.-J. Choi, A. Filer and J.-B. Baek, *J. Mat. Chem. A*, 2014, **2**, 12136-12149.
10. D. Gunlycke, D. Areshkin, J. Li, J. Mintmire and C. White, *Nano. Lett.*, 2007, **7**, 3608-3611.
11. M. Pumera, *Energy Environ. Sci.*, 2011, **4**, 668-674.
12. M.-Q. Zhao, Q. Zhang, J.-Q. Huang, G.-L. Tian, J.-Q. Nie, H.-J. Peng and F. Wei, *Nat. Commun.*, 2014, **5**, 1-8.
13. X. Wang and G. Shi, *Energy. Environ. Sci.*, 2015, **8**, 790-823.
14. M. Zhang and B.-C. Ye, *Chem. Commun.* , 2012, **48**, 3647-3649.
15. F. Schedin, A. K. Geim, S. V. Morozov, E. W. Hill, P. Blake, M. I. Katsnelson and K. S. Novoselov, *Nat. Mater.*, 2007, **6**, 652-655.
16. A. T. Lawal, *Tantala*, 2015, **131**, 424-443.
17. J. P. Rourke, P. A. Pandey, J. J. Moore, M. Bates, I. A. Kinloch, R. J. Young and N. R. Wilson, *Angew. Chem. Int. Ed.*, 2011, **50**, 3173-3177.
18. A. M. Dimiev and T. A. Polson, *Carbon*, 2015, **93**, 544-554.
19. M. Quintana, E. Vazquez and M. Prato, *Acc. Chem. Res.*, 2013, **46**, 138-148.
20. Z. Liu, J. T. Robinson, X. Sun and H. Dai, *J. Am. Chem. Soc.*, 2008, **130**, 10876-10877.
21. L. M. Veca, F. Lu, M. J. Meziani, L. Cao, P. Zhang, G. Qi, L. Qu, M. Shrestha and Y.-P. Sun, *Chem. Comm.*, 2009, 2565-2567.
22. H. J. Salavagione, M. A. Gómez and G. Martínez, *Macromolecules*, 2009, **42**, 6331-6334.
23. S. Niyogi, E. Bekyarova, M. E. Itkis, J. L. McWilliams, M. A. Hamon and R. C. Haddon, *J. Am. Chem. Soc.*, 2006, **128**, 7720-7721.
24. Y. Xu, Z. Liu, X. Zhang, Y. Wang, J. Tian, Y. Huang, Y. Ma, X. Zhang and Y. Chen, *Adv. Mater.*, 2009, **21**, 1275-1279.
25. C. G. Salzmann, V. Nicolosi and M. L. H. Green, *J. Mater. Chem.*, 2010, **20**, 314-319.
26. X. Jia, J. Campos-Delgado, M. Terrones, V. Meuniere and M. S. Dresselhaus, *Nanoscale*, 2011, **3**, 86-95.
27. X. Zhang, J. Xin and F. Ding, *Nanoscale*, 2013, **5**, 2556-2569.
28. H. P. Boehm, *Carbon*, 2002, **40**, 145-149.
29. A. Lerf, H. He, M. Forster and J. Klinowski, *J. Phys. Chem. B*, 1998, **102**, 4477-4482.

Please do not adjust margins
RSC Advances

ARTICLE

30. E. K. Fields and S. Meyerson, *Chem. Comm.*, 1965, 474-476.
31. S. C. Moldoveanu, in *Techniques and Instrumentation in Analytical Chemistry*, ed. C. M. Serban, Elsevier, 2010, vol. 28, pp. 471-526.
32. C. Moreno-Castilla, F. Carrasco-Marín, F. J. Maldonado-Hódar and J. Rivera-Utrilla, *Carbon*, 1998, **36**, 145-151.
33. J. L. Figueiredo, M. F. R. Pereira, M. M. A. Freitas and J. J. M. Órfão, *Carbon*, 1999, **37**, 1379-1389.
34. K. A. Hunter and P. S. Liss, *J. Electroanal. Chem.*, 1976, **73**, 347-358.

Please do not adjust margins

48x27mm (300 x 300 DPI)